

# Immunodeficiency virus uptake, turnover, and 2-phase transfer in human dendritic cells

Stuart G. Turville, John J. Santos, Ines Frank, Paul U. Cameron, John Wilkinson, Monica Miranda-Saksena, Joanne Dable, Hella Stössel, Nikolaus Romani, Michael Piatak Jr, Jeffrey D. Lifson, Melissa Pope, and Anthony L. Cunningham

**HIV-1 subverts antigen processing in dendritic cells (DCs) resulting in viral uptake, infection, and transfer to T cells. Although DCs bound monomeric gp120 and HIV-1 similarly, virus rarely colocalized with endolysosomal markers, unlike gp120, suggesting HIV-1 alters endolysosomal trafficking. Virus within DC intracellular compartments rapidly moved to DC-CD4<sup>+</sup> lymphocyte synapses when introduced to CD4<sup>+</sup> lymphocyte cultures.**

**Although viral harboring and transfer from nonlysosomal compartments was transient, given DC-associated virus protein, nucleic acids, and infectious HIV-1 transfer to CD4<sup>+</sup> lymphocytes decayed within 24 hours. However a second long-term transfer phase was apparent in immature DCs after 48 hours as a zidovudine-sensitive rise in proviral DNA. Therefore, DCs transfer HIV-1 to CD4<sup>+</sup> lymphocytes in 2 distinct phases. Immature and ma-**

**ture DCs first divert virus from the endolysosomal pathway to the DC-T-cell synapse. Secondly, the later transfer phase from immature DCs is through de novo HIV-1 production. Thus, the controversy of DCs being infected or not infected for the mechanics of viral transfer to CD4<sup>+</sup> lymphocytes can be addressed as a function of time. (Blood. 2004;103:2170-2179)**

© 2004 by The American Society of Hematology

## Introduction

The interactions of HIV-1 with dendritic cells (DCs) provide a paradox whereby DCs are crucial for mounting an effective immune response yet contribute to HIV-1 spread.<sup>1</sup> In animal models using simian immunodeficiency virus (SIV), infected DCs are observed early in the mucosa.<sup>2</sup> Infected DCs probably mediate virus spread to CD4<sup>+</sup> T cells, with subsequent virus amplification in these T cells.<sup>3,4</sup> Several studies sampling peripheral and lymphoid tissues from infected human subjects demonstrated viral replication within DCs *in vivo*.<sup>5-10</sup> HIV-1 also uses the intimate contact of DCs with CD4<sup>+</sup> lymphocytes<sup>11-14</sup> for transfer, resulting in explosive viral replication in DC-CD4<sup>+</sup> lymphocyte cocultures.<sup>11,13,14</sup> However, the underlying mechanisms have remained obscure.

Immature DCs, especially those in epithelia, recognize and ingest whole pathogens and/or their related antigens, transporting them between peripheral and lymphoid tissues linking the innate and acquired immune response in lymphoid tissue. Through such mechanisms HIV-1 may gain access to CD4<sup>+</sup> lymphocytes in lymphoid tissue.<sup>2-4,10,11</sup> The envelope glycoprotein of HIV-1 (gp120) is highly glycosylated with high mannose saccharides,<sup>15,16</sup> and virus attachment to DCs is mediated largely through mannose-specific C-type lectin receptors (CLRs).<sup>15-21</sup> Recent studies postu-

lated DC-SIGN (CD209) as the predominant CLR on DCs responsible for HIV-1 attachment.<sup>18</sup> However, in DCs of skin and stratified squamous mucosal epithelium, other CLRs may be at least as important for HIV-1 binding (Langerin [CD207] on epidermal Langerhans cells and mannose receptor [MR, CD206] on dermal DCs).<sup>20</sup> Immature DCs express higher levels of these CLRs than mature DCs, but both readily capture virions and hold them in distinct intracellular compartments.<sup>22,23</sup>

As CLRs do not mediate direct fusion of HIV-1 to the cell membrane like CD4/CCR5, the fate of bound virus might be predicted to be degradation via endolysosomal compartments.<sup>24,25</sup> Geijtenbeek et al<sup>18</sup> observed in DC-SIGN transfectants and monocyte-derived DCs (MDDCs) that virus could be captured and transferred to CD4<sup>+</sup> T cells by a mechanism called “*transinfection*.” This allows transfer of virus from a cell type that captures, but does not become infected, via DC-SIGN. The *transinfection* hypothesis has been extended to internalization and retention of intact infectious virus within DCs, with subsequent exit and transfer of virions (independent of DC infection).<sup>26</sup> However, it is still unclear how HIV-1 escapes degradation within the CLR-antigen processing pathway or whether it is bypassed. Although

From the Centre For Virus Research, Westmead Millennium Institute, Sydney, Australia; Center for Biomedical Research, Population Council, New York, NY; Department of Microbiology and Immunology, University of Melbourne, Parkville, Australia; the Department of Dermatology and Venereology, University of Innsbruck, Austria; and the AIDS Vaccine Program, Science Applications International Corporation (SAIC)–Frederick, National Cancer Institute at Frederick, Frederick, MD.

Submitted September 15, 2003; accepted October 17, 2003. Prepublished online as *Blood* First Edition Paper, November 20, 2003; DOI 10.1182/blood-2003-09-3129.

Supported by the Australian National Centre for HIV Virology Research (A.L.C.), an Australian Postgraduate Award (S.G.T.), and grant no. 991482 from the Australian National Health and Medical Research Council (P.U.C.), and equipment grants from the Wellcome trust and ANZ trustees (P.U.C.). M. Pope is an Elizabeth Glaser Scientist of the Elizabeth Glaser Pediatric AIDS Foundation. This work was funded by National Institutes of Health (NIH) grants

R21 AI52060, R01 AI40877, P01 HD41752, and AI52048, The Rockefeller Foundation, and the Elizabeth Glaser Pediatric AIDS Foundation (M.P.). H.S. and N.R. were supported by the Tyrolean Provincial Hospital Company (TILAK). This work was also supported in part with federal funds from the National Cancer Institute, NIH, under contract no. NO1-CO-124000 (J.D.L.).

S.G.T. and J.J.S. contributed equally to this work.

A.L.C. and M. Pope were equal senior contributors.

**Reprints:** A. L. Cunningham, Westmead Millennium Institute, PO Box 412, Darcy Rd, Westmead, NSW 2145, Australia; e-mail: tony\_cunningham@wmi.usyd.edu.au.

The publication costs of this article were defrayed in part by page charge payment. Therefore, and solely to indicate this fact, this article is hereby marked “advertisement” in accordance with 18 U.S.C. section 1734.

© 2004 by The American Society of Hematology

others have observed mechanisms of viral transfer quite separate from *trans*-infection, where they show the need for infection of DCs prior to transfer to CD4<sup>+</sup> lymphocytes.<sup>14,27-29</sup> This is consistent with selection of R5 HIV-1 during transmission, even when CLR-mediated enhancement of infection occurs in "*cis*."<sup>30</sup>

This study aimed at dissecting the intracellular fates and turnover of whole virus after binding to MDDCs by using concentrated HIV-1/SIV particles. We studied the stability and disposition of gp120 versus virions after uptake, and also characterized the ability of virus-pulsed DCs to transfer virus to CD4<sup>+</sup> T cells over time. In contrast to previous reports using CLR transfectants, both immature and mature MDDCs rapidly process and degrade virions in compartments lacking classical endolysosomal markers. The initial phase of transfer of virus from MDDCs to T cells is temporally limited by the degradation of virus via this pathway. Although, a second kinetic phase occurs that is dependent on productive infection of immature DCs, with transfer of progeny virus to T cells.

## Materials and methods

### Flow cytometry

The following antibodies were used: CD1a (HI149; Pharmingen, San Diego, CA), CD3 (Leu4; Becton Dickinson [BD], San Jose, CA), CD4 (Leu3a; BD), CD11c (LeuM5; BD), CD14 (LeuM3; BD), CD25 (2A3; BD), CD80 (L307.4; BD), CD83 (HB15e [Pharmingen] or HB15A [Immunotech, Marseille, France]), CD86 (IT2.2; Pharmingen), CD206 (Mannose Receptor, clone 3.29; Immunotech or Pharmingen), CD209 (DC-SIGN, clone 120507; R&D Systems, Minneapolis, MN), and HLA-DR (L243; BD).

### Immunofluorescence and confocal microscopy

The following antibodies were used: CD209 (clone 28 [AIDS Reagent Repository, NIH] and clone 120507 [R&D Systems]), CD206 (clone 19; Pharmingen), CD107b (lysosomal-associated membrane protein 2 [LAMP-2]; clone H4B4; Pharmingen), HLA-DR (L243; BD), early endosomal antigen 1 (EEA1; clone 14; BD Transduction Laboratories, San Jose, CA), HIV-1 p24 (OT34A; ICN, Costa Mesa, CA), and sheep polyclonal antibody to HIV-1 p24 (Cliniqa-Aalto, Fallbrook, CA).

### Primary leukocyte isolation

Leukopacks were obtained from the Sydney Blood Bank and the New York Blood Centre. Monocytes were isolated from peripheral blood by positive selection using CD14 magnetic beads (Miltenyi Biotech, Gladbach, Germany) as previously described.<sup>22</sup> Direct sorting yielded purities of 99% or more CD14<sup>+</sup> monocytes as assessed by flow cytometry (CD11c and CD14 staining). CD4<sup>+</sup> lymphocytes were sorted using the CD4 lymphocyte isolation kit or by depletion of HLA-DR<sup>+</sup>CD8<sup>+</sup>CD11b<sup>+</sup> cells (Miltenyi Biotech) ( $\geq$  98% purity; CD3, CD4, CD8, and HLA-DR staining).

### Primary cell cultures

Monocytes were converted to immature MDDCs by culture in granulocyte-macrophage colony-stimulating factor (GM-CSF) and interleukin-4 (IL-4) using 1 of 2 standard approaches that generate comparable DC populations with the characteristic phenotype (CD14<sup>+</sup>, MR, DC-SIGN, and CD1a high, negligible CD25, CD80, CD83, moderate CD86, and HLA-DR).<sup>19,22,23</sup> To obtain mature MDDCs, cells were cultured for 2 more days in a cocktail of prostaglandin E2 ( $10^{-6}$  M; Sigma, St Louis, MO), tumor necrosis factor  $\alpha$ , IL-1 $\beta$ , and IL-6 (10 ng/mL; R&D Systems).<sup>22</sup> Mature DCs up-regulate CD25, CD80, CD83, CD86, and HLA-DR, and down-regulate MR and DC-SIGN. CD4<sup>+</sup> lymphocytes were activated with phytohemagglutinin (PHA, 5  $\mu$ g/mL; Sigma) for 2 days, washed, and cultured in 20 U/mL IL-2 (Roche Molecular Biochemicals, Indianapolis, IN).

### HIV-1 gp120 labeling strategies

Purified HIV-1<sub>BaL</sub> gp120 (NIH AIDS Research and Reference Reagent Program) was biotinylated to allow detection using fluorochrome-conjugated streptavidin. For biotinylation of carbohydrates on gp120, HIV-1 gp120 saccharide residues were oxidized by adding freshly prepared sodium metaperiodate (Sigma) to gp120 to give a final concentration of 15 mM. The gp120 was left to oxidize on ice for 30 minutes with no light. The oxidation reaction was stopped by adding glycerol to a final concentration of 15 mM. Excess sodium metaperiodate and glycerol were removed by dialysis overnight against phosphate-buffered saline (PBS). Biotin-LC-hydrazide (Pierce, Rockford, IL) was dissolved in dimethyl sulfoxide (DMSO; Sigma) at 50 mM and added to oxidized gp120 to a final concentration of 5 mM. Labeling proceeded at room temperature with agitation for 2 hours, and excess biotin-LC-hydrazide was removed by extensive dialysis.

### Generation of concentrated chemically inactivated HIV-1 and SIV

Aldrithiol-2 (AT-2) SIV isolates (SIV E11S or SIV CP-mac) and HIV-1<sub>ADA</sub> were provided by the AIDS Vaccine Program (SAIC-Frederick, National Cancer Institute at Frederick, Frederick, MD) and prepared as previously described.<sup>22,31-33</sup> Infectious HIV-1<sub>BaL</sub> was generated in PHA-activated peripheral blood mononuclear cell (PBMC)-PM1 (NIH AIDS Research and Reference Reagent Program) cocultures and were similarly purified and treated or not with AT-2 under comparable conditions. Virus content of purified concentrated preparations was determined using p27 or p24 *gag* enzyme-linked immunosorbent assay (ELISA) and/or by high-performance liquid chromatography (HPLC) analysis, as described,<sup>32</sup> and stocks were stored at  $-80^{\circ}\text{C}$ .

### Quantitation of viral transfer from MDDCs to CD4<sup>+</sup> lymphocytes

A quantitative assay measuring early DC to T-cell viral transfer events was performed by pulsing immature MDDCs for 2 hours with HIV-1 (0.1 proviral forming units per cell as measured in PM1 cells after a 2-hour viral pulse and proviral DNA quantification 24 hours after infection by real-time quantitative polymerase chain reaction [Q-PCR]). MDDCs were thoroughly washed 3 times in cold PBS supplemented with 1% human serum and 2 mM EDTA (ethylenediaminetetraacetic acid) and cultured in IL-4/GM-CSF media. At indicated times,  $5 \times 10^4$  MDDCs ( $50 \mu\text{L}$  IL-4/GM-CSF) were incubated with  $2 \times 10^5$  PHA-activated allogeneic CD4<sup>+</sup> lymphocytes ( $150 \mu\text{L}$  containing 10 U/mL IL-2). DC-T-cell cocultures were harvested 24 hours after DC addition by washing in PBS, pelleting, and storing at  $-70^{\circ}\text{C}$  until Q-PCR analysis. To control for the contribution of DC-associated proviral copies, pure virus-pulsed immature MDDCs were cultured and analyzed in parallel. The contribution of DCs to HIV-1 DNA in cocultures was shown to be minor compared with CD4<sup>+</sup> lymphocytes, as DC depletion from cocultures had relatively little effect on total HIV DNA. Use of a short-term assay to measure early virus transfer events avoids many of the problems of experimental variability seen in longer term cocultures.

### Loading DCs with HIV-1 gp120 and AT-2 viruses

Prior to use,  $1 \times 10^6$  cells/mL were pulsed with gp120 (10  $\mu\text{g}/\text{mL}$ , 30 minutes at  $37^{\circ}\text{C}$  in IL-4/GM-CSF) and washed. MDDCs were mixed with AT-2 HIV-1 (2-3  $\mu\text{g}$  of p24/ $10^6$  cells) or AT-2 SIV (0.3  $\mu\text{g}$  of p27/ $10^6$  cells), and the cell-virus mixtures were incubated for 30 to 60 minutes. After washing,<sup>22</sup> cells were sampled immediately (0 hours) or after reculture in IL-4/GM-CSF (immature DCs) or regular medium (mature DCs) ( $0.5 \times 10^6/\text{mL}$ ). At each time point,  $2 \times 10^5$  cells were washed in PBS and dry cell pellets were stored at  $-70^{\circ}\text{C}$  until p24 analysis. Alternatively, DCs were loaded with AT-2 SIV, washed, and the presence of virus monitored 0 to 24 hours later by microscopy or reverse-transcription (RT)-PCR.<sup>22</sup> Cells were also cultured in medium, GM-CSF/IL-4, or the maturation cocktail ( $0.5-1 \times 10^6$  cells/well of a 24-well plate in 1.5 mL).

## Quantitative PCR

Quantitative PCR for HIV-1 LTR-*gag* DNA and estimation of cell numbers by CCR5 DNA copy number were performed using primers and molecular beacons as previously described.<sup>34</sup> RT-PCR for SIV *gag* RNA was performed as previously described.<sup>22</sup>

## Cell-associated p24 ELISA

Cell pellets from AT-2 HIV-1-pulsed MDDCs were lysed at a concentration of  $3 \times 10^5$  cells/mL in 1% (vol/vol) nonidet-P40/Triton X-100 with 10 mM HEPES (*N*-2-hydroxyethylpiperazine-*N'*-2-ethanesulfonic acid), 0.14 M NaCl, 10 mM MgCl<sub>2</sub> plus protease inhibitors, 10 mM tosyl arginyl methyl ester, 1 mM phenylmethylsulfonyl fluoride (PMSF), 10 μg/mL leupeptin and aprotinin, 100 μg/mL soybean trypsin inhibitor, and 10 mM dithiothreitol (DTT) (all from Sigma). HIV-1 p24 was quantified by HIV-1 p24 ELISA (Beckman-Coulter, Hialeah, FL).

## Immunofluorescent microscopy

DCs ( $5 \times 10^4$ ) pulsed with biotinylated gp120 or AT-2 HIV-1 were either cytospun onto glass slides using a cytospin centrifuge (Shandon Thermo, Woburn, MA) or adhered to alcian blue-treated slides.<sup>22</sup> Cells were either fixed and permeabilized in acetone ( $-20^\circ\text{C}$ , 15 minutes) or 4% paraformaldehyde with saponin-permeabilization and then stained using streptavidin Alexa Fluor 594 (5 μg/mL; Molecular Probes, Eugene, OR), murine monoclonal primary antibodies (5 μg/mL), and secondary goat antimouse Alexa Fluor 488 (5 μg/mL; Molecular Probes) or stained for virus envelope using biotinylated human CD4-immunoglobulin G<sub>2</sub> (IgG<sub>2</sub>) (provided by William C. Olson, Progenics Pharmaceutical, Tarrytown, NY) and the fluorescein-labeled trichostatin A (TSA) kit amplification reagent (NEN, Boston, MA).<sup>22</sup> To detect viral and cellular antigens concurrently, murine monoclonal primary antibodies (versus isotype controls) were added with biotinylated CD4-IgG<sub>2</sub> and bound antibodies detected with the Alexa Fluor 594-conjugated goat anti-mouse Ig. Nuclei were stained with DAPI (4,6 diamidino-2-phenylindole, D-1306, 1.75 ng/mL; Molecular Probes). Slides were then mounted using fluorescent mounting medium (DAKO, Carpinteria, CA) and examined using either a Leica TCS SP2 laser scanning spectral confocal microscope (Leica Microsystems AG, Wetzlar, Germany) at  $\times 643$  magnification or a Nikon Eclipse E800 epifluorescence microscope with the Image-Pro Plus deconvolution module (Media Cybernetics, Silver Spring, MD).

## Transmission electron microscopy

Cells were fixed in modified Karnovsky fixative for 1 hour, with fixed samples, processed, and ultra-thin sections examined following a previously published protocol.<sup>22</sup>

## Coculture of virus-loaded DCs with T cells for visualization of virus transfer

AT-2 virus-pulsed DCs were mixed with autologous resting or PHA-activated CD4<sup>+</sup> T cells (1 DC/4 T cells in 100 μL) in serum-free medium, centrifuged (30 seconds, 500 rpm), and incubated to allow conjugate formation (30 minutes, ice). Cells were then incubated at 37°C for 0 to 2 hours before being gently resuspended and adhered to alcian blue-treated slides. After fixation and permeabilization, virus envelope was detected using biotinylated CD4-IgG<sub>2</sub> combined with anti-HLA-DR-phycoerythrin (PE) staining and nuclei staining with DAPI.

## Results

### HIV-1 gp120 labeling strategies for tracking in DCs

We previously demonstrated binding of biotinylated HIV-1 gp120 to DCs by flow cytometry<sup>19,20</sup> by labeling primary amines of gp120 with biotin *N*-hydroxysuccinimide (NHS) esters. To enhance sensitivity for immunofluorescence microscopy we used biotin-LC-

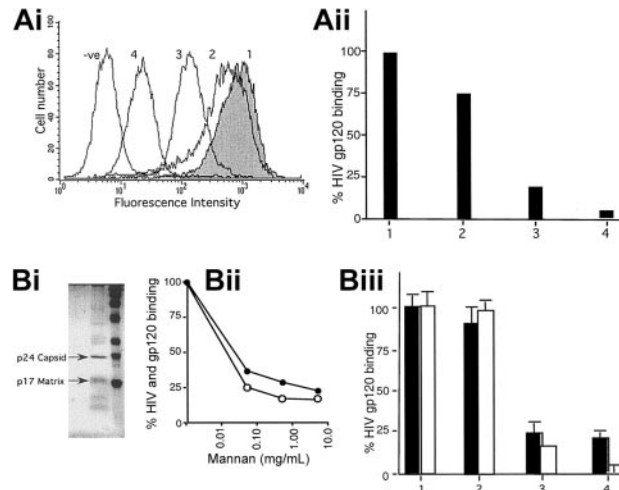


**Figure 1. HIV-1 gp120 and HIV-1 purification for attachment and tracking studies in MDDCs.** (A) Binding specificity of biotin-LC-hydrazide gp120. (Ai) Specific binding of labeled gp120 to CLR and CD4 was examined by preincubating MDDCs with either the CLR inhibitor mannan at 5 mg/mL, the CD4 mAb Leu3a at 10 μg/mL, or a combination of both prior to the addition of gp120. Flow cytometry of cells incubated under the following conditions are shown. (1) Media alone (filled gray panel), (2) Leu3a, (3) mannan, (4) Leu3a and mannan. Untreated cells were included for comparison (-ve). (Aii) Inhibition of HIV gp120 binding for each condition described for panel Ai was compared as percent gp120 binding. Mean fluorescence intensities (MFIs) were converted into percent binding by the following formulas: [(MFI of gp120 binding in the presence of inhibitors) - (MFI background (no gp120))] / [(MFI of the gp120 binding positive control (no inhibitors)) - (MFI background)]. (B) AT-2 HIV-1<sub>BaL</sub> purification and binding to MDDCs. (Bi) AT-2 HIV-1<sub>BaL</sub> was velocity-gradient purified as described in "Materials and methods," and 5 μg HIV-1 p24 was lysed and diluted 1:2 in 1 × loading dye and subjected to SDS-PAGE and staining by Coomassie blue. Major protein bands p24 (capsid) and p17 (matrix) are indicated by arrows (left gel lane). Molecular weight markers are shown in the right lane. (Bii) Percent AT-2 HIV-1 and HIV-1 gp120 binding were compared in the presence of increasing concentrations of the CLR inhibitor, mannan. For detection of HIV-1 attachment,  $1 \times 10^5$  cells/100 μL were preincubated with mannan for 1 hour and then 2 μg/mL p24 of purified virus at 4°C for 1 hour. Cells were washed, pelleted, and lysed and virus p24 was detected by ELISA. Percent HIV binding was calculated as follows: (sample - negative control)/(positive control). Negative control was media alone for HIV and gp120 binding. Positive controls were virions and gp120 binding in the absence of inhibitors for HIV and gp120, respectively. ●, gp120; ○, HIV-1 virions. (Biii) Inhibition of AT-2 HIV-1 (■; p24 ELISA) and gp120 (□; flow cytometry) binding to MDDCs was compared in the presence of (1) media alone, (2) Leu3a, (3) mannan, and (4) mannan and Leu3a as in panel Ai. All results shown are representative of at least 3 experiments. Error bars indicate standard deviation.

hydrazide to biotinylate gp120 via carbohydrates (Figure 1). Biotin-LC-hydrazide-labeled gp120 detected with a streptavidin fluorophore conjugate allowed ready detection of bound gp120 in flow cytometric assays (Figure 1Ai). Inhibition of binding to CLR and CD4 by blockade with the oligomannose saccharide, mannan, and the anti-CD4 mAb, Leu3a, demonstrated that binding was specific and similar to previous results with other labeled gp120 preparations (Figure 1Aii). Furthermore, biotin-LC-hydrazide labeling of gp120 also facilitated its intracellular detection by fluorescence microscopy (Figure 2).

### HIV-1 gp120 binding specificity correlates with that of purified HIV-1

Mannan-inhibitable binding of labeled monomeric gp120 to DCs was compared with binding of whole virus (Figure 1Bi). AT-2 viruses are not infectious, but retain conformationally, and functionally intact, fusion competent gp120, and behave comparably with infectious virions with respect to binding and uptake by target cells.<sup>22,33</sup> As previously reported for gp120,<sup>19,20</sup> AT-2 HIV-1<sub>BaL</sub> attachment to CLR at 4°C was inhibited in a dose-dependent manner by mannan (Figure 1Bii). As there was

residual binding even with excess mannan (approximately 1 mg/mL), combined inhibition with mannan and anti-CD4 was used to determine if there were 2 phases of binding as observed with gp120.<sup>19,20</sup> This combination did not further inhibit the residual binding (Figure 1Biii). Thus, there is a third (< 20%) mechanism of binding of HIV-1 to MDDCs, independent of CD4 and mannan.

### Disposition of HIV-1 gp120 in immature MDDCs

As HIV-1 binding to immature MDDCs and its inhibition by mannan is similar to binding of gp120, we initially used biotinylated gp120 to evaluate the internal transport pathway of HIV-1. After 30 minutes of addition, gp120 colocalized with MR and to a lesser extent with DC-SIGN located subjacent to the plasma membrane within vesicles (Figure 2Ai). The patterns of LAMP-2, MR, and DC-SIGN stains were not changed by uptake of gp120 (Figure 2Ai-ii). After 120 minutes, gp120 entered deeper LAMP-2<sup>+</sup> compartments, colocalizing with MR but dissociating from DC-SIGN, which remained at the periphery (Figure 2Aiii). To distinguish the relative roles of MR and DC-SIGN in uptake, immature DCs were treated with trypsin to remove DC-SIGN, while leaving MR still capable of binding gp120 (Figure 2B).<sup>19</sup> HIV gp120 bound and entered trypsin-treated MDDCs (Figure 2B-D) and colocalized with MR in endosomes and later with MR and LAMP-2 (Figure 2Ci-ii) similar to nontrypsinized cells (Figure 2A). To confirm trafficking of gp120 with MR but not DC-SIGN, cells were analyzed for surface receptor expression at serial times after entry of gp120. Both MR and CD4 were progressively down-regulated immediately after the 30-minute pulse and further after the 120-minute

chase (Figure 2D). In contrast, there was no significant decrease in DC-SIGN expression, consistent with the observations by confocal microscopy that MR and gp120, but not DC-SIGN, track to lysosomes.

### Binding and trafficking of AT-2 HIV-1/SIV in MDDCs

We next compared the binding and disposition of whole virions with monomeric gp120. AT-2 virus is captured and internalized by MDDCs like infectious virus, but the intracellular sequestration of virus is different between immature and mature DCs.<sup>22,23</sup> Therefore, we compared binding and internalization of HIV-1<sub>BaL</sub> gp120 (Figure 2) versus AT-2 HIV-1<sub>BaL</sub> (not shown), HIV-1<sub>ADA</sub> (Figure 3), and SIV (Figure 4B-C) in immature and mature MDDCs. After 30 to 60 minutes of exposure to AT-2 HIV-1 (Figure 3) or SIV (not shown), protein was detected in cytoplasmic vesicular compartments. As with SIV<sup>22</sup> (Figure 4B), HIV-1 envelope staining concentrated at the periphery of immature DCs (Figure 3A,C) and deeper in larger vesicles as a “spot” in mature DCs (Figure 3B). Unlike monomeric gp120, whole virus rarely colocalized with any of the markers tested (EEA1, LAMP-2, MR, DC-SIGN) immediately after the virus pulse (0h) or after a 2-hour chase (2h). Similar observations were made using AT-2 SIV (not shown). Different SIV and HIV-1 isolates were handled similarly by DCs.

### Degradation of AT-2 virus in MDDCs

To examine the stability of internalized virions, MDDCs were pulsed with AT-2 HIV-1<sub>BaL</sub> and cell-associated viral p24 was measured over time. Progressive loss of p24 occurred, with

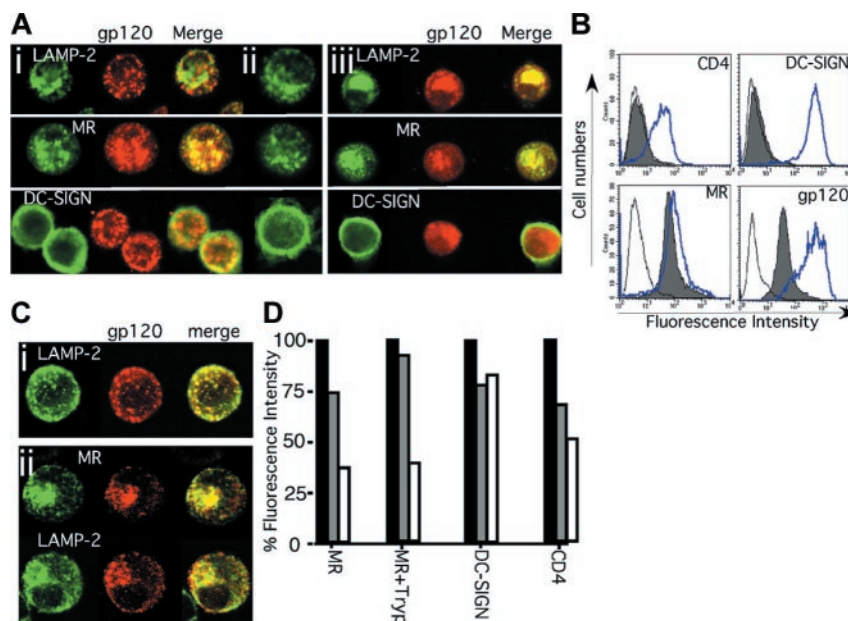


**Figure 2. Internalization of HIV-1 gp120 by immature MDDCs.** The binding and entry of HIV-1 gp120 into immature MDDCs was examined using excess biotin-LC-hydrazide gp120. Original magnification,  $\times 400$ . After a 30-minute pulse with gp120 (Ai) or no gp120 (Aii) or a subsequent 120-minute chase (Aiii),  $5 \times 10^4$  cells were cytospun onto glass slides and fixed in 4°C acetone for 10 minutes. HIV-1 gp120 was detected using streptavidin Alexa Fluor 594 (red) and fluorescent colocalization examined with monoclonal antibodies to the lysosome marker LAMP-2 and the 2 CLR, MR and DC-SIGN (green), by confocal microscopy. (Similar results were observed with alcian blue–adhered, paraformaldehyde-fixed, and saponin-permeabilized MDDCs stained with biotinylated CD4-IgG<sub>2</sub>.) (B) MDDCs were trypsinized, resulting in cleavage of the gp120 binding domains of functional CD4 (Leu3a) and DC-SIGN (AZN-D1) but not completely of MR. Solid gray histograms represent antibody (or streptavidin) staining for CD4, DC-SIGN, MR, and gp120 after trypsinization, and the open overlaid histograms represent their respective isotype or negative (no gp120) controls. The blue open overlaid histograms show respective staining in each panel before trypsinization. (C) HIV-1 gp120 uptake into different trypsinized MDDCs at 0 (Ci) and 120 (Cii) minutes after gp120 loading was detected as outlined for panel A. (D) Cell surface expression of MR on untreated (MR) or trypsinized MDDCs (MR+Tryp) and expression of DC-SIGN and CD4 (on untreated cells) was determined immediately before the gp120 pulse (before gp120; ■), immediately after the 30-minute pulse (0 minutes; □), and after a 120-minute chase (120 minutes; □). Percent fluorescence intensity = MFI as a proportion of control.

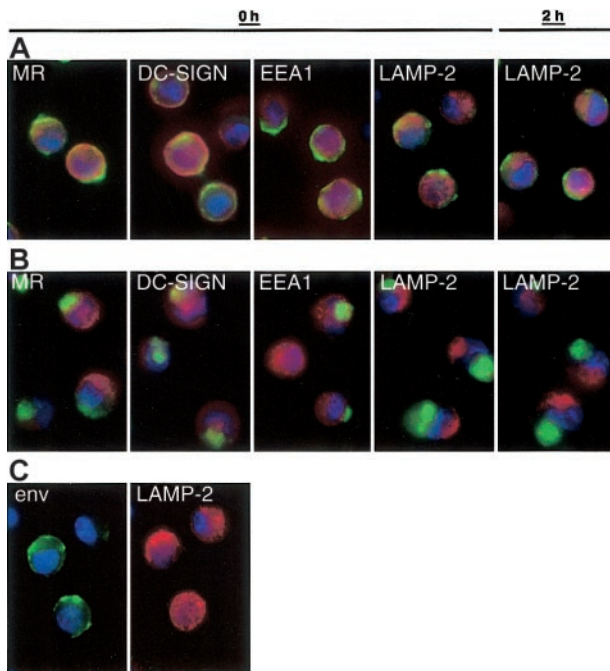


**Figure 3. Internalization pathways of virus in mature and immature MDDCs.** Immature (A,C) and mature (B) MDDCs were incubated with AT-2 HIV-1<sub>ADA</sub> ( $3 \mu\text{g}$  p24/10<sup>6</sup> DCs, 1 hour at 37°C) and free virus was washed away. The cells were gently resuspended, and approximately  $2.5 \times 10^4$  cells adhered to alcian blue-treated slides immediately (0 h) or after an additional 2-hour incubation (2 h). Cells were fixed in 4% paraformaldehyde and incubated with biotinylated CD4-IgG<sub>2</sub> (Progenics Pharmaceutical) in addition to murine monoclonals specific for MR, DC-SIGN, EEA1, and LAMP-2 at room temperature in the presence of saponin. After washing, bound biotinylated CD4-IgG<sub>2</sub> was detected with streptavidin-horseradish peroxidase (HRP) and HRP located using the FITC-TSA amplification kit (green).<sup>22</sup> Murine monoclonals were detected with goat antimouse Alexa Fluor 594 (red) and nuclei were stained with DAPI (blue). Overlays of the green and red stains are shown in panels A and B. Separate stains for envelope (env) and LAMP-2 on immature DCs (0 h as an example) are shown in panel C to highlight the limited colocalization of these stains. Original magnification  $\times 100$ . Double staining for LAMP-2 or MR and envelope was reproduced using 8 different donors, and DC-SIGN and EEA1 repeated with 5 donors. Comparable results were obtained using AT-2 SIV CP-mac-loaded DCs from 2 additional donors (not shown). Murine Ig isotype controls showed no background staining with goat antimouse Alexa Fluor 594 (not shown).

biphasic kinetics in mature and immature MDDCs. The approximate half-life of p24 in immature DCs was 4 hours and 4.5 hours for mature MDDCs (Figure 4Ai). From 6 to 24 hours there was a slower phase of p24 decay in both cell populations. Examination of p24 distribution within immature DCs by confocal microscopy showed loading of HIV-1 into vesicles (as seen with envelope, Figure 3), subjacent to the membrane (Figure 4Aii). After 6 hours, multiple small p24<sup>+</sup> vesicles were detected in the cell periphery. Although these vesicles persisted until 24 hours, they gradually faded over time and were fewer in number than those observed at 6 hours, suggesting there was progressive degradation of HIV-1 in vesicular compartments. From 24 to 72 hours there was little detectable p24 in MDDCs (Figure 4Ai). Similar quantitative declines were seen for cell-associated SIV gag RNA measured by real-time RT-PCR in DCs pulsed with AT-2 SIV (not shown).

To visualize SIV degradation, AT-2 SIV-loaded DCs were examined for the expression of virus envelope immediately (0d) or 1 day (1d) after being recultured in medium alone or medium supplemented with GM-CSF/IL-4 or the maturation cocktail (Figure 4B). As with AT-2 HIV-1, the numbers of envelope<sup>+</sup> cells (and the intensity of staining) reduced over time. This was

particularly apparent in immature DCs when viewing low-power fields (Figure 4Bi, top panels). Cells retaining viral proteins showed a similar cellular distribution with time (Figure 4Bi, bottom panels), small vesicles around the immature DC periphery and the deeper spotlike stain in mature DCs that still did not costain with EEA1, LAMP-2, MR, or DC-SIGN (not shown). Even if virus was acquired by immature DCs, subsequent exposure to an external maturation stimulus resulted in virus protein staining appearing in a more localized spot within the cells (much like mature DCs; Figure 4Bii). When DCs were only partially matured prior to virus exposure (one day of the maturation stimulus), virus captured by these cells was distributed in smaller more peripheral vesicles (such as immature DCs) as well as the more concentrated (mature) localization (Figure 4Bii, upper panels). As soon as these cells were recultured under any condition, virus localized to a concentrated area within the cells, mirroring the matured DC profile.

Electron microscopic analysis of 24-hour cultured cells revealed that residual viral proteins (and RNA) coincided with less intact virions being visible (Figure 5). Intact SIV particles were observed in large vacuoles within mature DCs (Figure 5A-C), although fewer than directly after initial uptake.<sup>22</sup> Fragmented structures possibly representing cellular debris or degraded virions were also observed (Figure 5B-C, asterisks). Similar results were seen in DCs from 4 different donors, a total of 150 different cell profiles. In immature DCs, virus is located in smaller vesicles positioned just underneath the cell membrane immediately after exposure.<sup>22</sup> Although more rare, SIV (Figure 5D-F) and HIV-1 (not shown) particles (both intact and possibly degraded) were still evident in 24-hour cultured immature DCs. These observations were made on DCs from 2 different donors, a total of 100 different cell profiles. Residual protein stains (Figure 4A-B) probably reflect intact virions as well as partially degraded virus seen by electron microscopy. The combination of protein detection, PCR, and electron microscopy indicates that virus captured by DCs is degraded with time and the fate of virus within the cell is readily influenced by external stimuli.

#### T-cell contact triggers virus movement to the DC-T-cell synapse

External stimuli (above) and T cells<sup>12</sup> influence the intracellular fate of virions trapped by DCs. Using AT-2 virus we monitored the transmission of virus between virus-bearing DCs and autologous CD4<sup>+</sup> T cells. To synchronize events, virus-pulsed DCs were mixed with T cells and DC-T-cell contact was encouraged by centrifugation and incubation for 30 minutes at 4°C (to avoid virus movement) prior to incubation at 37°C. DC-T-cell conjugates were observed after 30 minutes at 4°C. Typically, DC-T-cell conjugates represent 5% to 10% of the cocultures at any time point (estimated on slides and quantified by flow cytometry, not shown). Within 1 hour of DC-T-cell contact at 37°C, staining for SIV (Figure 6, arrows) or HIV-1 (not shown) proteins showed a striking localization to DC-T-cell synapses, compared with the distribution in virus-carrying single DCs (or DCs cultured alone in parallel; Figures 3-4). Virus movement to contact points occurred in all donors examined but only at 37°C (not at 4°C). The kinetics of movement to the synapses varied between donors yet was always apparent within 30 to 60 minutes of culture at 37°C. Despite more conjugates in mature DC-T-cell mixtures (approximately 2-fold), virus protein staining at DC-T-cell synapses occurred with both immature and mature DCs.

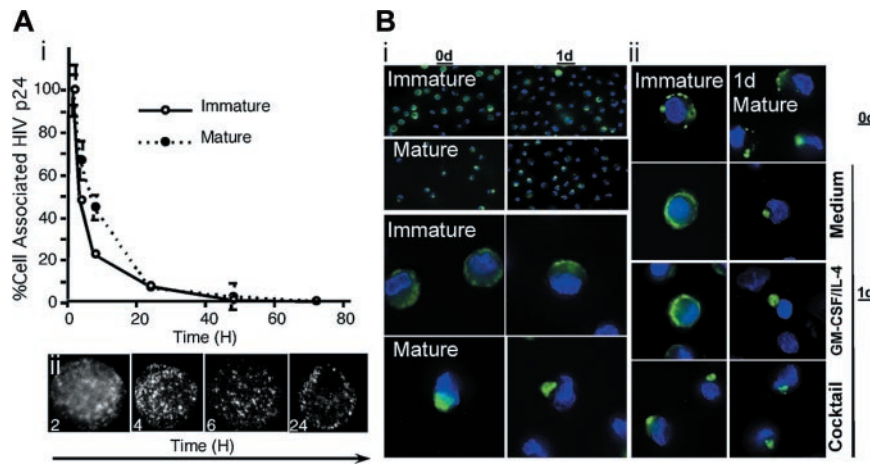


**Figure 4. Viral degradation in both immature and mature DCs.** (A) Quantitative decay of intracellular HIV p24. (Ai) Purified AT-2 HIV-1<sub>BAL</sub> was incubated with immature and mature MDDCs ( $1 \times 10^6$  cells/mL,  $2 \mu\text{g/mL}$  HIV-1 p24) for 2 hours. Cells were washed 3 times and cultured at  $0.5 \times 10^6$  cells/mL in IL-4/GM-CSF media. At the indicated times, cells were pelleted for cell-associated p24 quantified as for Figure 1. At time 0 hours, immediately following the pulse, cell-associated p24 was  $18 \text{ ng p24}/10^6$  for immature DCs and  $5 \text{ ng p24}/10^6$  for mature DCs. The p24 amounts measured at each time point are expressed as a percentage relative to the 100% starting points and are representative of 3 experiments. (Aii) Alternatively, cytospin preparations were made at the indicated time points and acetone-fixed on glass. AT-2 HIV-1 was detected using a murine anti-HIV-1 p24 monoclonal antibody followed by Alexa 488-conjugated goat anti-mouse IgG. At the 6- and 24-hour time points, exposure was enhanced 3-fold to demonstrate the presence of fluorescent granules. Original magnification,  $\times 100$ . (B) Degradation of SIV (envelope) in DCs over 24 hours. (Bi) AT-2 SIV CP-mac-loaded immature or mature DCs were sampled immediately (0 d) or after being recultured for 1 day (1 d) ( $10^6$  cells/well, 24-well plate; immature in GM-CSF/IL-4 and mature in medium alone) adhered to slides. Cells were stained for SIV envelope and nuclei using biotinylated CD4-IgG<sub>2</sub> and DAPI, respectively, as outlined in Figure 3. A low-power image (i, upper panels; original magnification,  $\times 10$ ) and a higher-power deconvoluted Z series image (i, lower panels; original magnification,  $\times 100$ ) are shown. Data are representative of DCs from 7 donors. (Bii) Immature DCs and cells matured for one day in cocktail (1d Mature) were pulsed with AT-2 SIV E11S ( $30 \text{ ng p27}/10^5$  DCs, 2 hours at  $37^\circ\text{C}$ ) and sampled immediately (0 d) or recultured in the presence of medium, GM-CSF/IL-4, or the maturation cocktail for a day (1d). Cells were adhered to slides and stained for envelope expression. Immature and 1-day matured DCs yielded the same results from 5 different individuals. Original magnification,  $\times 100$ . Comparative analyses confirmed the similarities between the different SIV isolates (as apparent in panels Bi and Bii).

Virus staining was detected on single T cells as well as on T cells in DC-T-cell conjugates remote from the contact region (Figure 6, asterisks), consistent with virus/viral proteins being transferred to lymphocytes. Although difficult to quantify, there was a consistent relative increase in the numbers of virus-positive single T cells as well as virus staining between adjacent

T cells with time (Figure 5, arrowheads), further supporting the notion of DCs handing virus to T cells that continue to spread virus among themselves. Similar movement of HIV-1 proteins to synapses between DCs and activated CD4<sup>+</sup> T cells and onto T cells was observed (not shown). Therefore, in agreement with recent findings using labeled virions,<sup>12</sup> we found that AT-2

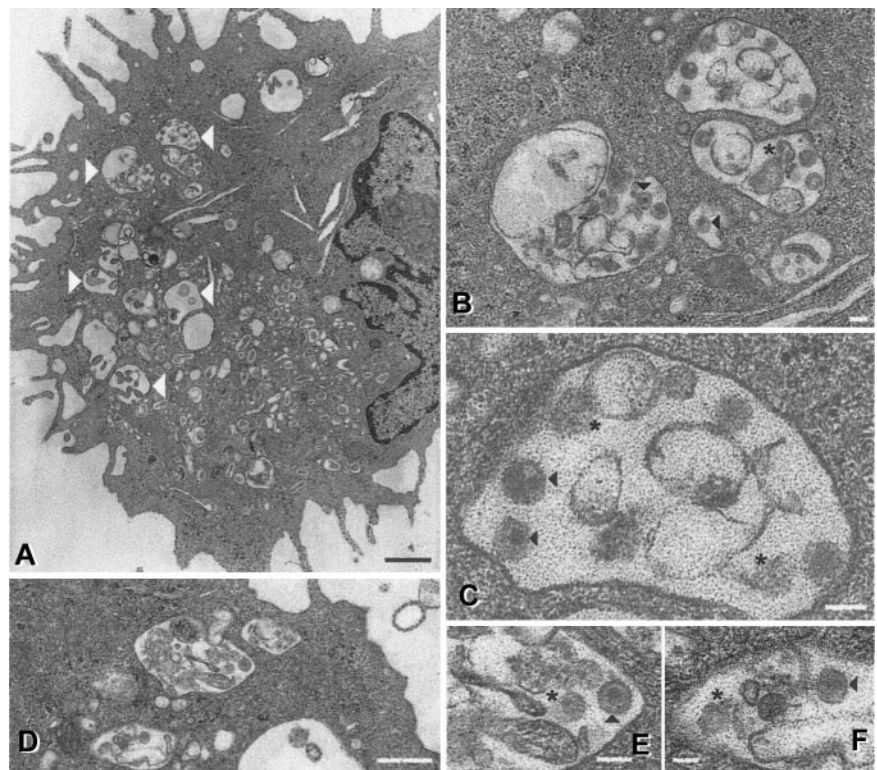


**Figure 5. Ultrastructural appearance of SIV particles in DCs after 24 hours.** Mature and immature DCs were pulsed with AT-2 SIV CP-mac for 2 hours, washed, and cultured for an additional 24 hours (immature DCs in GM-CSF and IL-4 and mature DCs in regular medium). At the 24-hour time point, cells were fixed and processed for electron microscopy as previously described.<sup>22</sup> In mature DCs (A-C) large vacuoles (large white arrowheads) containing intact particles (black arrowheads) and cellular debris or possible degraded virions (asterisks) were observed. Similar virions (as well as debris or degraded viral particles) were observed in immature DCs (D-F), although at a markedly lower frequency. Magnifications and scale bars: (A)  $\times 9000$ ,  $2 \mu\text{m}$ ; (B)  $\times 31\,000$ ,  $100 \text{ nm}$ ; (C)  $\times 81\,000$ ,  $10 \text{ nm}$ ; (D)  $\times 23\,000$ ,  $0.5 \mu\text{m}$ ; (E)  $\times 60\,000$ ,  $100 \text{ nm}$ ; (F)  $\times 51\,000$ ,  $100 \text{ nm}$ . These images represent observations from 2 donors for the immature DCs and 4 donors for the mature DCs.

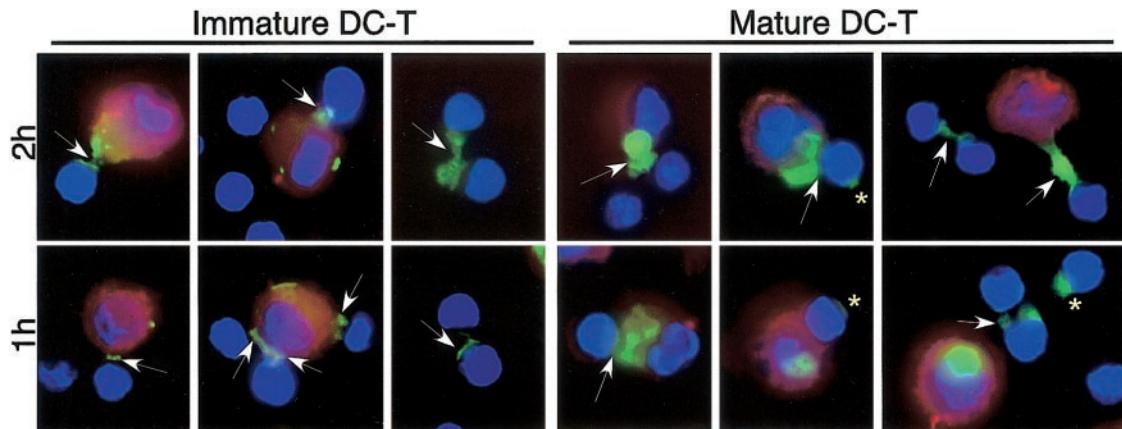


**Figure 6. Viral transfer from MDDCs to CD4<sup>+</sup> lymphocytes.** Immature or mature MDDCs were exposed to AT-2 SIV CP-mac, and cell-free virus was washed away. AT-2 SIV-bearing DCs were mixed with autologous CD4<sup>+</sup> T cells, centrifuged, and incubated to allow conjugate formation. The cells were then incubated at 37°C for 1 or 2 hours (5-7 donors) before the cells were adhered to alcian blue-treated slides. Staining for SIV envelope (green) and cellular nuclei (blue) was performed as outlined in Figure 3. DCs were identified by staining with PE-conjugated anti-HLA-DR (red). Arrows show transfer of SIV envelope between DCs and T cells, and arrowheads denote cell-to-cell transmission between T cells. Asterisks show SIV envelope on T cells, often remote from the DC-T-cell synapse. Virus staining at the DC-T-cell synapses was seen in all donors after incubation at 37°C, but the extended virus-positive "bridges" between DCs and T cells were observed more infrequently. Murine and human Ig controls showed no staining. Original magnification,  $\times 100$ .

viruses move to DC-T-cell synapses, to facilitate virus amplification in resting and activated CD4<sup>+</sup> T cells.

#### Two phases of infectious HIV-1 transfer to CD4<sup>+</sup> T cells

The capacity to transfer infectious virus to CD4<sup>+</sup> lymphocytes over time was examined in an attempt to delineate the need for DC infection versus direct transfer in the absence of DC infection (ie, *Trans*-infection). DCs were exposed to infectious HIV-1<sub>BaL</sub> and cultured for varying lengths of time before being cultured with CD4<sup>+</sup> T cells. Full-length proviral DNA was quantified over 72 hours together with simultaneous measurement of cell-associated p24 and virus transfer from DCs to CD4<sup>+</sup> lymphocytes (proviral DNA in cocultures minus input DNA from infected DCs after 24 hours after the addition of DCs).

Initially, quantitative transfer of HIV-1 from immature MDDCs to CD4<sup>+</sup> lymphocytes directly correlated with p24 decay. From 0 to 24 hours there was good correlation during first phase of decay kinetics, extending to the early part of the second phase (Figures 4Ai and 7A). However, during the second phase from 24 to 72 hours there was divergence between the 2 curves. HIV-1 p24 declined to undetectable levels, but a second phase of viral transfer increased rapidly from 48 to 72 hours, coinciding with an increase in proviral DNA in pure immature MDDC cultures (Figure 7A). Treatment of DCs with the antiretroviral reverse-transcriptase inhibitor, zidovudine, prior to addition to the T cells did not impact the first phase of transfer, but abrogated the second transfer phase as well as the replication within DCs cultured alone (Figure 7B). In contrast in mature MDDCs, there was an initial decay in viral transfer as seen in immature DCs, which plateaued after 24 hours (Figure 7C), followed by a progressive decrease from 48 to 72 hours. Therefore, the first phase of viral transfer from immature and mature MDDCs is independent of *de novo* HIV-1 replication within the DCs, while the second phase is dependent on the ability of immature DCs to complete *de novo* viral production (Figure 7D).

## Discussion

The critical yet opposing roles DCs play in HIV-1 infection<sup>1</sup> emphasize the need to elucidate the underlying mechanisms. We

identified several novel features of DC-virus biology that help explain how DCs augment infection while undermining immunity. This biology was confirmed comparing live and AT-2 HIV-1 and SIV (versus gp120), highlighting the similarities between HIV-1/SIV handling by DCs as well as the usefulness of AT-2 virus to study early events in virus-cell interplay and cell-to-cell transmission. We found that while virus and monomeric gp120 are similarly captured by MDDCs, virus is diverted from classical endolysosomal processing machinery. In spite of this, significant amounts of virus are degraded within 24 hours, coinciding with decreased ability to transmit captured virus to T cells across DC-T-cell synapses. Residual virus is infectious and immature DCs exhibit a second phase of increased transmissibility as they facilitate virus replication for transfer to T cells (Figure 7D).

Initial studies using monomeric gp120 revealed that gp120 binds predominantly to CLRs (MR, DC-SIGN) on immature MDDCs, while in mature MDDCs these CLRs are down-regulated and CD4 binding predominates.<sup>19,20</sup> AT-2 HIV-1, expressing native gp120, similarly binds immature DCs via CLR-dominant mechanisms. Minor binding to another unknown receptor(s) seems likely since 10% to 20% binding remained after blocking CD4 and CLRs. MDDCs that were trypsin-depleted of surface DC-SIGN internalized gp120, colocalizing with MR, and gp120 internalization depleted surface MR (but not DC-SIGN), suggesting that MR may be more important for uptake or an existing redundancy between the 2 CLRs. A specific neutralizing ligand for MR is needed to distinguish between these alternatives. The receptor mediating internalization in mature DCs is yet to be defined. Furthermore, gp120 and MR (not DC-SIGN) traffic to lysosomes. Internalization into endosomes would be expected to be similar since both CLRs contain tyrosine-based motifs for internalization in clathrin-coated vesicles and undergo endosomal trafficking.<sup>35</sup> DC-SIGN expressed in THP1 cells is internalized after ligand exposure<sup>26</sup> and DC-SIGN expressed in HeLa cells promotes HIV-1 internalization.<sup>36</sup> Caution must be applied in extrapolating results from transfected cell lines to primary human DCs as expression of endolysosomal proteins and MR differs. Also studies of MR trafficking seem contradictory and may depend on its bound ligands. Mannose-bovine serum albumin (BSA) enters early endosomes but recycles to the plasma membrane, avoiding trafficking to lysosomes and degradation.<sup>35</sup>

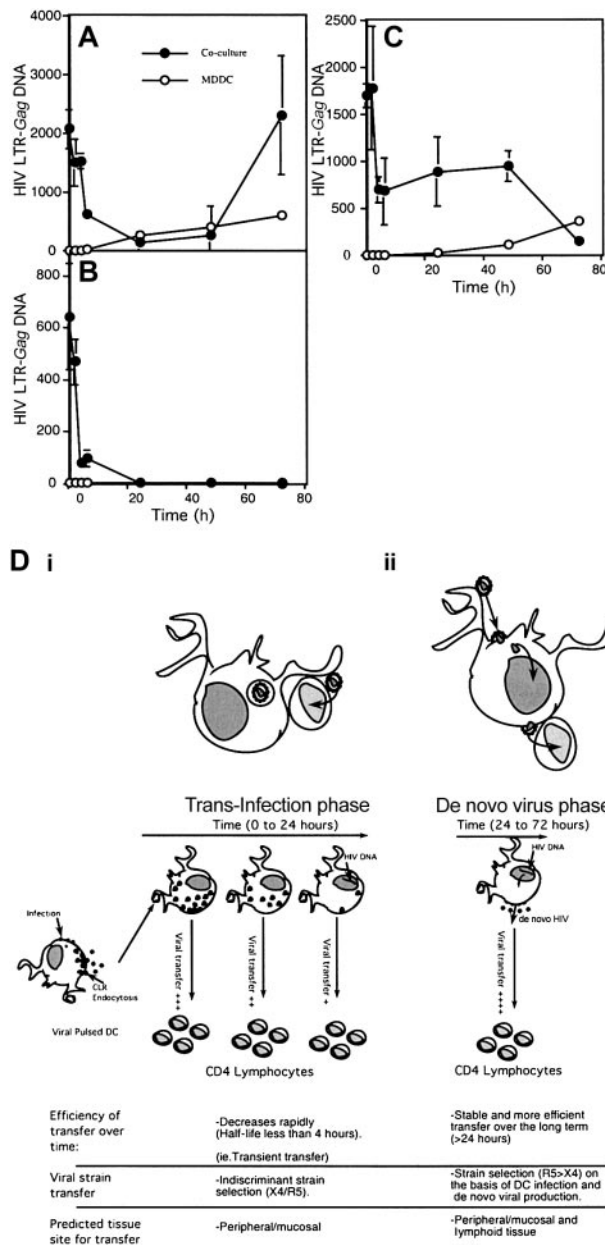


**Figure 7. Phases of HIV transfer from MDDCs to CD4 T cells.** Both immature MDDCs (A-B) and mature MDDCs (C) were treated with infectious HIV-1<sub>Bal</sub> for 2 hours and washed. MDDCs were then cultured in IL-4/GM-CSF media for varying time points. In panel B, MDDCs were cultured in the presence of 10 μM zidovudine. MDDCs at indicated time points were washed, harvested by pelleting, and resuspended in IL-4/GM-CSF media and then cultured with PHA-activated CD4<sup>+</sup> T cells in a ratio of 1 DC to 4 CD4<sup>+</sup> T cells. At 24 hours after mixing of the cells, the combined cell pellet was lysed and assayed for full-length HIV-1 DNA by Q-PCR. Pure cultures of MDDCs were also harvested at the same time points to determine DNA levels in DCs alone. The DNA input into the cocultures by DCs was subtracted from coculture HIV-1 DNA and is presented as HIV-1-LTR gag DNA per 1 × 10<sup>6</sup> cells. HIV-1-LTR gag DNA in 0.2 × 10<sup>6</sup> DCs is also presented in overlaid graphs in open circles. In panel D, a model of transfer from immature MDDCs to CD4<sup>+</sup> lymphocytes over time is illustrated on the basis of results in upper panels A-B. In panels Di-ii, the characteristics of both phases of HIV-1 transfer from MDDCs to CD4<sup>+</sup> lymphocytes are shown. The first phase (i) results from diversion of infectious virus from the endolysosomal pathway of degradation (“trans-infection”). The proposed second phase (ii) of de novo viral production in DCs (“cis” infection) prior to transfer to CD4<sup>+</sup> lymphocytes. Note that this phase is stable and consistent with R5 HIV-1 strain selection initially observed in vivo HIV-1 transmission.

However lipoarabinomannan, a microbial ligand rich in oligomannose residues such as gp120, colocalizes with MR in late endosomes or lysosomes.<sup>24</sup> DC-SIGN may recycle, similar to the internalization pathway proposed for MR after mannose-BSA

ligation in MDDCs. This is supported by the restoration of DC-SIGN surface expression after ligand exposure.<sup>37</sup> Virus is held in distinct locations within immature and mature DCs,<sup>22</sup> but, unlike gp120, rarely colocalized with MR or DC-SIGN in either population, suggesting that they must release the virus rapidly after internalization.

Early colocalization of HIV-1 with transferrin receptor and the presence of HIV-1 in clathrin-coated vesicles confirms uptake into the endosomal pathway.<sup>22,26</sup> In further contrast to gp120, virus rarely colocalized with classical endolysosomal markers in DCs, in agreement with others.<sup>26</sup> Whole virus may interfere with normal endolysosomal traffic, comparable with inhibition by other intracellular pathogens such as mycobacteria.<sup>38</sup> While immature DCs often took up more virus than mature DCs,<sup>22</sup> rapid decay of virus protein and RNA was evident in both, although typically slower and less complete in mature DCs. Thus, transport to LAMP-2<sup>+</sup> lysosomes may not be necessary for viral degradation as late endosomes still contain highly proteolytic activity.<sup>39</sup> Compared with mature DCs, immature DCs possess a greater capacity for antigen uptake,<sup>40</sup> yet mature DCs exhibit enhanced lysosomal activity augmenting antigen processing and formation of major histocompatibility complex II (MHC II) peptides, coinciding with more potent immunostimulatory function.<sup>41</sup> Although at least some virus captured by immature and mature DCs can be presented to virus-specific T cells,<sup>42,43</sup> it is possible that most virions avoid classical lysosomal antigen processing, thereby subverting the activation of strong antiviral immunity. The lack of virus localization in LAMP-2<sup>+</sup> vesicles 30 to 150 minutes after virus addition supports this.

Previous reports of virus internalization by DCs and transfer to T cells emphasized transfer of infectious virus soon after internalization without replication,<sup>12,18,26,44,45</sup> while others focused on amplification within DCs.<sup>27-29,46</sup> Our current results resolve the apparent contradictions in these data by showing that immature MDDCs transfer virus to T cells via 2 different mechanistically and kinetically distinct processes (Figure 7D). Transfer of infectious virus shortly after uptake does not require de novo synthesis of new virus and diminishes rapidly with time (Figure 7Di). Retarded levels of viral degradation in mature MDDCs likely explain the residual “first phase” viral transfer that is not seen in immature MDDCs. The second phase of transfer is delayed for 1 to 2 days following initial uptake and can be inhibited by zidovudine, indicating that this is dependent on productive infection of immature MDDCs (Figure 7Dii).

DC-to-T-cell spread of HIV-1 requires cell-cell contact<sup>47</sup> and envelope-dependent interactions with chemokine receptors on T cells.<sup>48</sup> Recent studies demonstrated rapid movement of fluorescently tagged virus from DCs to CD4<sup>+</sup> T cells, where CD4, CCR5, and CXCR4 were recruited on T cells at the DC contact point. This underscored how DCs can efficiently facilitate virus spread to CD4<sup>+</sup> T cells. Complementing these observations, we demonstrated viral proteins accumulating at DC-T-cell synapses when AT-2 virus-loaded DCs contact resting or activated CD4<sup>+</sup> T cells and increasing amounts of virus on T cells with time, indicative of DC-to-T-cell spread. Further support for virus movement was provided by electron microscopic documentation of virion accumulation at DC-T-cell synapses (not shown). In agreement with McDonald et al,<sup>12</sup> this occurred with immature and mature DCs, with mature DCs more readily forming DC-T-cell conjugates than immature DCs even in the absence of specific antigen. These data provide direct evidence for how DC-T-cell conjugates drive HIV-1



infection.<sup>13</sup> Movement of tubular MHC II peptide-bearing compartments to contact points between DCs and peptide-specific T cells was recently reported.<sup>49,50</sup> Virus may exploit this machinery to spread from DCs to CD4<sup>+</sup> T cells, and especially immature DCs to virus-specific T cells.<sup>51</sup>

The identification of the 2 distinct phases of HIV-1 transfer to CD4<sup>+</sup> lymphocytes in immature MDDCs and primarily first phase transfer in mature MDDCs has interesting *in vivo* implications. After contact of cell-free or cell-associated HIV-1 in genital secretions with immature epithelial DCs, the first phase might occur with resting CD4<sup>+</sup> lymphocytes within healthy tissues.<sup>52</sup> Transfer between immature and mature DCs and resting and activated T cells would likely be enhanced in inflamed tissues (eg, inflammation caused by pathogens such as herpes simplex virus). This transfer should be nonselective for X4 or R5 viruses and mainly mediated via CLRs. Earlier studies reported no first phase of transfer independent of DC infection,<sup>27-29</sup> possibly due to the time at which DCs encounter T cells (skin DCs exposed to HIV-1 were obtained days after HIV-1 exposure following emigration<sup>27,29</sup>). Therefore, the "window of opportunity" for HIV-1 to escape from endolysosomal destruction by CD4<sup>+</sup> lymphocyte engagement would have passed. This may also explain the selective R5 HIV-1 transmission to CD4<sup>+</sup> lymphocytes, which would not occur when the first phase of (indiscriminant) transfer

occurs. The second phase of transfer through immature DC replication of virus may predominate *in vivo*, resulting in selective transmission and persistence of R5 isolates in early infection<sup>52,53</sup> and amplification in the mucosa and lymph nodes. This is best illustrated by individuals homozygous for a 32-base pair deletion in CCR5 being highly resistant to HIV-1 transmission.<sup>53</sup> Notably, CCR5/CD4-dependent infection versus CD4/CLR-dependent capture and dissemination of virus was recently described for mucosal DCs using the human cervical explant model (J. Hu et al, manuscript submitted, 2003). The precise role of all relevant receptors, including currently identified and yet-to-be-identified CLRs, should be studied as it is critical for the development of antiviral agents able to block transmission.

## Acknowledgments

The following reagents were obtained through the AIDS Research and Reference Reagent Program, Division of AIDS, National Institute of Allergy and Infectious Diseases (NIAID), NIH: HIV-1 BaL gp120 from Division of AIDS (DAIDS), NIAID; DC-SIGN monoclonal antibody (DC28) from Drs F. Baribaud, S. Pöhlmann, J. A. Hoxie, and R. W. Doms; and PM1 from Dr Marvin Reitz.

## References

- Frank I, Pope M. The enigma of dendritic cell-immunodeficiency virus interplay. *Curr Mol Med*. 2002;2:229-248.
- Hu J, Gardner MB, Miller CJ. Simian immunodeficiency virus rapidly penetrates the cervicovaginal mucosa after intravaginal inoculation and infects intraepithelial dendritic cells. *J Virol*. 2000;74:6087-6095.
- Stahl-Hennig C, Steinman RM, Tenner-Racz K, et al. Rapid infection of oral mucosal-associated lymphoid tissue with simian immunodeficiency virus. *Science*. 1999;285:1261-1265.
- Zhang Z, Schuler T, Zupancic M, et al. Sexual transmission and propagation of SIV and HIV in resting and activated CD4<sup>+</sup> T cells. *Science*. 1999;286:1353-1357.
- Bhoopat L, Eiangleng L, Ruggao S, et al. *In vivo* identification of Langerhans and related dendritic cells infected with HIV-1 subtype E in vaginal mucosa of asymptomatic patients. *Mod Pathol*. 2001;14:1263-1269.
- Cimarelli A, Zambruno G, Marconi A, Girolomoni G, Bertazzoni U, Giannetti A. Quantitation by competitive PCR of HIV-1 proviral DNA in epidermal Langerhans cells of HIV-infected patients. *J Acquir Immune Defic Syndr*. 1994;7:230-235.
- Dusserre N, Dezutter-Dambuyant C, Mallet F, et al. *In vitro* HIV-1 entry and replication in Langerhans cells may clarify the HIV-1 genome detection by PCR in epidermis of seropositive patients. *J Invest Dermatol*. 1992;99:99S-102S.
- Frankel SS, Wenig BM, Burke AP, et al. Replication of HIV-1 in dendritic cell-derived syncytia at the mucosal surface of the adenoid. *Science*. 1996;272:115-117.
- Hu J, Miller CJ, O'Doherty U, Marx PA, Pope M. The dendritic cell-T cell milieu of the lymphoid tissue of the tonsil provides a locale in which SIV can reside and propagate at chronic stages of infection. *AIDS Res Hum Retroviruses*. 1999;15:1305-1314.
- Spira AI, Marx PA, Patterson BK, et al. Cellular targets of infection and route of viral dissemination after an intravaginal inoculation of simian immunodeficiency virus into rhesus macaques. *J Exp Med*. 1996;183:215-225.
- Cameron PU, Freudenthal PS, Barker JM, Gezelter S, Inaba K, Steinman RM. Dendritic cells exposed to human immunodeficiency virus type-1 transmit a vigorous cytopathic infection to CD4<sup>+</sup> T cells. *Science*. 1992;257:383-387.
- McDonald D, Wu L, Bohks SM, KewalRamani VN, Unutmaz D, Hope TJ. Recruitment of HIV and its receptors to dendritic cell-T cell junctions. *Science*. 2003;300:1295-1297.
- Pope M, Betjes MG, Romani N, et al. Conjugates of dendritic cells and memory T lymphocytes from skin facilitate productive infection with HIV-1. *Cell*. 1994;78:389-398.
- Pope M, Gezelter S, Gallo N, Hoffman L, Steinman RM. Low levels of HIV-1 infection in cutaneous dendritic cells promote extensive viral replication upon binding to memory CD4<sup>+</sup> T cells. *J Exp Med*. 1995;182:2045-2056.
- Leonard CK, Spellman MW, Riddle L, Harris RJ, Thomas JN, Gregory TJ. Assignment of intrachain disulfide bonds and characterization of potential glycosylation sites of the type 1 recombinant human immunodeficiency virus envelope glycoprotein (gp120) expressed in Chinese hamster ovary cells. *J Biol Chem*. 1990;265:10373-10382.
- Zhu X, Borchers C, Bienstock RJ, Tomer KB. Mass spectrometric characterization of the glycosylation pattern of HIV-gp120 expressed in CHO cells. *Biochemistry*. 2000;39:11194-11204.
- Curtis BM, Scharnowske S, Watson AJ. Sequence and expression of a membrane-associated C-type lectin that exhibits CD4-independent binding of human immunodeficiency virus envelope glycoprotein gp120. *Proc Natl Acad Sci U S A*. 1992;89:8356-8360.
- Geijtenbeek TB, Kwon DS, Torensma R, et al. DC-SIGN, a dendritic cell-specific HIV-1-binding protein that enhances trans-infection of T cells. *Cell*. 2000;100:587-597.
- Turville SG, Arthos J, Mac Donald K, et al. HIV gp120 receptors on human dendritic cells. *Blood*. 2001;98:2482-2488.
- Turville SG, Cameron PU, Handley A, et al. Diversity of receptors binding HIV on dendritic cell subsets. *Nat Immunol*. 2002;3:975-983.
- Turville SG, Cameron PU, Hart DN, Cunningham AL. C-type lectin-HIV attachment on dendritic cells: innate immune recognition and processing or mediators of HIV transmission? *Trends Glycosci Glycotech*. 2002;14:255.
- Frank I, Piatak M Jr, Stoessel H, et al. Infectious and whole inactivated simian immunodeficiency viruses interact similarly with primate dendritic cells (DCs): differential intracellular fate of virions in mature and immature DCs. *J Virol*. 2002;76:2936-2951.
- Frank I, Pope M. Consequences of dendritic cell (DC)-immunodeficiency virus interactions: chemically inactivated virus as a model for studying antigen presentation and virus transmission by primate DCs. *Immunobiology*. 2001;204:622-628.
- Prigozy TI, Sieling PA, Clemens D, et al. The mannose receptor delivers lipoglycan antigens to endosomes for presentation to T cells by CD1b molecules. *Immunity*. 1997;6:187-197.
- Sallusto F, Cella M, Danieli C, Lanzavecchia A. Dendritic cells use macropinocytosis and the mannose receptor to concentrate macromolecules in the major histocompatibility complex class II compartment: downregulation by cytokines and bacterial products. *J Exp Med*. 1995;182:389-400.
- Kwon DS, Gregorio G, Bitton N, Hendrickson WA, Littman DR. DC-SIGN-mediated internalization of HIV is required for trans-enhancement of T cell infection. *Immunity*. 2002;16:135-144.
- Kawamura T, Cohen SS, Borris DL, et al. Candidate microbicides block HIV-1 infection of human immature langerhans cells within epithelial tissue explants. *J Exp Med*. 2000;192:1491-1500.
- Kawamura T, Gulden FO, Sugaya M, et al. R5 HIV productively infects Langerhans cells, and infection levels are regulated by compound CCR5 polymorphisms. *Proc Natl Acad Sci U S A*. 2003;100:8401-8406.
- Reece JC, Handley AJ, Anstee EJ, Morrison WA, Crowe SM, Cameron PU. HIV-1 selection by epidermal dendritic cells during transmission across human skin. *J Exp Med*. 1998;187:1623-1631.
- Lee B, Leslie E, Soilleux E, et al. Cis expression of DC-SIGN allows for more efficient entry of human and simian immunodeficiency viruses via

- CD4 and a coreceptor. *J Virol.* 2001;75:12028-12038.
31. Benveniste RE, Hill RW, Eron LJ, et al. Characterization of clones of HIV-1 infected HuT 78 cells defective in gag gene processing and of SIV clones producing large amounts of envelope glycoprotein. *J Med Primatol.* 1990;19:351-366.
  32. Chertova E, Bess JW Jr, Crise BJ, et al. Envelope glycoprotein incorporation, not shedding of surface envelope glycoprotein (gp120/SU), is the primary determinant of SU content of purified human immunodeficiency virus type 1 and simian immunodeficiency virus. *J Virol.* 2002;76:5315-5325.
  33. Rossio JL, Esser MT, Suryanarayana K, et al. Inactivation of human immunodeficiency virus type 1 infectivity with preservation of conformational and functional integrity of virion surface proteins. *J Virol.* 1998;72:7992-8001.
  34. Lewin SR, Vesanen M, Kostrikis L, et al. Use of real-time PCR and molecular beacons to detect virus replication in human immunodeficiency virus type 1-infected individuals on prolonged effective antiretroviral therapy. *J Virol.* 1999;73:6099-6103.
  35. Engering AJ, Cella M, Fluitsma D, et al. The mannose receptor functions as a high capacity and broad specificity antigen receptor in human dendritic cells. *Eur J Immunol.* 1997;27:2417-2425.
  36. Nobile C, Moris A, Porrot F, Sol-Foulon N, Schwartz O. Inhibition of human immunodeficiency virus type 1 Env-mediated fusion by DC-SIGN. *J Virol.* 2003;77:5313-5323.
  37. Engering A, Geijtenbeek TB, van Vliet SJ, et al. The dendritic cell-specific adhesion receptor DC-SIGN internalizes antigen for presentation to T cells. *J Immunol.* 2002;168:2118-2126.
  38. Hart PD, Young MR, Gordon AH, Sullivan KH. Inhibition of phagosome-lysosome fusion in macrophages by certain mycobacteria can be explained by inhibition of lysosomal movements observed after phagocytosis. *J Exp Med.* 1987;166:933-946.
  39. Pillay CS, Elliott E, Dennison C. Endolysosomal proteolysis and its regulation. *Biochem J.* 2002;363:417-429.
  40. Watts C, Amigorena S. Antigen traffic pathways in dendritic cells. *Traffic.* 2000;1:312-317.
  41. Trombetta ES, Ebersold M, Garrett W, Pypaert M, Mellman I. Activation of lysosomal function during dendritic cell maturation. *Science.* 2003;299:1400-1403.
  42. Larsson M, Fonteneau J-F, Lirvall M, Haslett P, Lifson JD, Bhardwaj N. Activation of HIV specific CD4 and CD8 T cells by human dendritic cells: roles for crosspresentation and non-infectious HIV-1 virus. *AIDS.* 2002;16:1319-1329.
  43. Frank I, Santos JJ, Mehlhop E, et al. Mature dendritic cells efficiently capture, process, and present chemically inactivated SIV to CD4 and CD8 T cells in vitro. *J AIDS.* 2003;34:7-19.
  44. Blauvelt A, Asada H, Saville MW, et al. Productive infection of dendritic cells by HIV-1 and their ability to capture virus are mediated through separate pathways. *J Clin Invest.* 1997;100:2043-2053.
  45. Dybul M, Weissman D, Rubbert A, et al. The role of dendritic cells in the infection of CD4+ T cells with the human immunodeficiency virus: use of dendritic cells from individuals homozygous for the delta32CCR5 allele as a model. *AIDS Res Hum Retroviruses.* 1998;14:1109-1113.
  46. Granelli-Piperno A, Delgado E, Finkel V, Paxton W, Steinman RM. Immature dendritic cells selectively replicate macrophagetropic (M-tropic) human immunodeficiency virus type 1, while mature cells efficiently transmit both M- and T-tropic virus to T cells. *J Virol.* 1998;72:2733-2737.
  47. Tsunetsugu-Yokota Y, Yasuda S, Sugimoto A, et al. Efficient virus transmission from dendritic cells to CD4+ T cells in response to antigen depends on close contact through adhesion molecules. *Virology.* 1997;239:259-268.
  48. Ketas TJ, Frank I, Klasse PJ, et al. Human immunodeficiency virus 1 (HIV-1) attachment, coreceptor and fusion inhibitors are active against both direct and trans infection of primary cells. *J Virol.* 2003;77:2762-2767.
  49. Boes M, Cerny J, Massol R, et al. T-cell engagement of dendritic cells rapidly rearranges MHC class II transport. *Nature.* 2002;418:983-988.
  50. Chow A, Toomre D, Garrett W, Mellman I. Dendritic cell maturation triggers retrograde MHC class II transport from lysosomes to the plasma membrane. *Nature.* 2002;418:988-994.
  51. Doue DC, Brenchley JM, Betts MR, et al. HIV preferentially infects HIV-specific CD4+ T cells. *Nature.* 2002;417:95-98.
  52. Zhu T, Mo H, Wang N, et al. Genotypic and phenotypic characterization of HIV-1 patients with primary infection. *Science.* 1993;261:1179-1181.
  53. Liu R, Paxton WA, Choe S, et al. Homozygous defect in HIV-1 coreceptor accounts for resistance of some multiply-exposed individuals to HIV-1 infection. *Cell.* 1996;86:367-377.